Cavity-Correlated Electron-Nuclear Dynamics from First Principles

Johannes Flick and Prineha Narang

Phys. Rev. Lett. **121**, 113002 — Published 12 September 2018

DOI: 10.1103/PhysRevLett.121.113002

Cavity correlated electron-nuclear dynamics from first principles

Johannes Flick* and Prineha Narang†
John A. Paulson School of Engineering and Applied Sciences, Harvard University, Cambridge, MA, USA
(Dated: August 23, 2018)

The rapidly developing and converging fields of polaritonic chemistry and quantum optics necessitate a unified approach to predict strongly-correlated light-matter interactions with atomic-scale resolution. Towards this overarching goal, we introduce a general time-dependent density-functional theory to study correlated electron, nuclear and photon interactions on the same quantized footing. We complement our theoretical formulation with the first *ab initio* calculation of a correlated electron-nuclear-photon system. For a CO_2 molecule in an optical cavity, we construct the infrared spectra exhibiting Rabi splitting between the upper and lower polaritonic branches, time-dependent quantum-electrodynamical observables such as the electric displacement field, and observe cavity-modulated molecular motion. Our work opens an important new avenue in introducing *ab initio* methods to the nascent field of collective strong vibrational light-matter interactions.

Remarkable experiments at the interface of condensed matter physics, quantum chemistry, and quantum optics have sparked recent interest in understanding strongly correlated electronic, nuclear, and electromagnetic field degrees of freedom induced by strong light-matter coupling. Experimentally different regimes including optomechanics in picocavities [1], vibrational ultra-strong coupling for chemical systems [2], strong coupling of surface plasmon polaritons and molecular vibrations [3], the anomalous Raman response under strong light-matter coupling [4], thermodynamics of strongly coupled molecules [5], and the change of the reaction rates under strong-light matter coupling [6] have been explored. Theoretically, such strong coupling has been analyzed for cavity-controlled chemistry via a polaron-decoupling [7], vibrationally dressed polaritons [8], changes in potential-energy surfaces [9, 10], spectroscopy [11] or changes in the ground-state under ultrastrong coupling [12].

Recently, first-principles methods such as density-functional theory (DFT) including time-dependent density-functional theory (TDDFT) have been generalized to the realm of correlated electron-photon interactions. This quantum-electrodynamical density-functional theory (QEDFT) [13–16] treats electrons and photons on the same quantized footing. As an exact reformulation of the Schrödinger equation, QEDFT can predict exactly correlated electron-photon dynamics in full real-space [16], linking closely with experimental observables. QEDFT has been shown to correctly capture correlated electron-photon systems [17, 18], but so far has not been demonstrated for problems in strong vibrational-photon coupling as observed in recent experiments [1–3, 6]. Yet, vibrational effects play a critical role in chemical reactions, for example, the altering the vibrational mode by strong light-matter coupling has been demonstrated to directly influence the reaction [6] potentially allowing for a site-selective chemistry. Since in strong vibrational-photon coupling experiments, the vibrational energies are on the same order of magnitude as the cavity mode, theory requires treating both on the same level of theory [19]. To computationally capture the correlated nature of the electron-nuclear interaction, many different approaches have been pursued in a DFT framework [20–27]. However, none of these methods include quantized electromagnetic fields which are essential for cavity correlated effects [28].

We close this critical gap and present a comprehensive theory that is capable of treating electron-nuclear-photon systems on the same quantized footing. In this paper, we discuss an important generalization of QEDFT to the realm of nuclear interactions with strong implications for experiments in cavity-driven molecule-light interactions.

The general setup of the theory is as follows. The matter component of the correlated system contains n_e electrons and $N_N = \sum_{I=1}^{K} N_I$ nuclei. With K we specify the number of different nuclei species, each containing N_I nuclei. We define a nuclei species I by common charge Z_I and mass M_I. If a nuclear species contains more than one nucleus, these particles are physically indistinguishable, as is the case for more than one electron. The matter component of the system is coupled to $\mathcal{N}$ quantized electromagnetic field (photon) modes. In the nonrelativistic limit, length-gauge, and dipole approximation [29], the dynamics of the system is given by the following time-dependent Schrödinger equation [19]

$$i\frac{\partial}{\partial t}\Psi(\underline{\mathbf{r}},\underline{\mathbf{R}},\underline{q},t) = \hat{H}(t)\Psi(\underline{\mathbf{r}},\underline{\mathbf{R}},\underline{q},t), \tag{1}$$

with initial state $\Psi_0(\underline{\mathbf{r}},\underline{\mathbf{R}},\underline{q},t_0)$, where we introduce the following notation for the electronic coordinates $\underline{\mathbf{r}} = (\mathbf{r}_1,...,\mathbf{r}_{n_e})$, the nuclear coordinates $\underline{\mathbf{R}} = (\mathbf{R}_{1,1},...,\mathbf{R}_{K,N_K})$, and the photon coordinates $\underline{q} = (q_1,...,q_{\mathcal{N}})$, respectively.

The Hamiltonian of the full problem is given by $\hat{H}(t) = \hat{H}_0 + \hat{H}_{\text{ext}}(t)$, where $\hat{H}_0$ describes the internal Hamiltonian of the different subsystems and their interactions, and $\hat{H}_{\text{ext}}(t)$ allows to control the entire system using external

classical variables. Let us first specify

$$\hat{H}_{\text{ext}}(t) = \int d\mathbf{r}\, v_{\text{ext}}(\mathbf{r},t)\hat{n}(\mathbf{r}) + \sum_{I=1}^{K} \mathbf{F}_{\text{ext}}^{(I)}(t)\cdot\mathbf{R}_I + \sum_{\alpha=1}^{\mathcal{N}} \frac{j_{\text{ext}}^{(\alpha)}(t)}{\omega_\alpha}\hat{q}_\alpha. \quad (2)$$

Hereby we have defined the external potential v_{ext} that couples to the electron density

$$n(\mathbf{r},t) = \left\langle \Psi(t)\middle|\sum_{i=1}^{n_e}\delta(\mathbf{r}-\mathbf{r}_i)\middle|\Psi(t)\right\rangle. \quad (3)$$

where the many-body wave function $\Psi(t)$ is the solution to Eq. 1. The classical force $\mathbf{F}_{\text{ext}}^{(I)}(t)$ couples to

$$\mathbf{R}_I(t) = \left\langle \Psi(t)\middle|\sum_{\beta=1}^{N_I}\mathbf{R}_{I,\beta}\middle|\Psi(t)\right\rangle. \quad (4)$$

For every species in the system, $\mathbf{R}_I$ corresponds to the center-of-mass motion of that species. If the species contains more than a single nucleus, we find a system of indistinguishable particles where the individual $\mathbf{R}_{I,\beta}$ can not be told apart and only the center of mass motion is measurable [30]. Finally, the classical time-derivative of a current $j_{\text{ext}}^{(\alpha)}(t)$ couples to the photon displacement coordinate

$$q_\alpha(t) = \langle\Psi(t)|\,\hat{q}_\alpha\,|\Psi(t)\rangle\,, \quad (5)$$

which is connected to the mode-resolved physical observables of the field, i.e. the electric displacement field $\hat{\mathbf{D}}_\alpha(\mathbf{x}) = \sqrt{4\pi}\omega_\alpha\boldsymbol{\lambda}_\alpha(\mathbf{x})\hat{q}_\alpha$. For the following discussion, we assume the internal Hamiltonian $\hat{H}_0$ as

$$\hat{H}_0 = \sum_{i=1}^{n_e} -\frac{\vec{\nabla}_i^2}{2} + \sum_{i>j}\frac{1}{|\mathbf{r}_i-\mathbf{r}_j|} + \hat{H}_p + \sum_{I=1}^{K}\sum_{\beta=1}^{N_I} -\frac{\vec{\nabla}_{I,\beta}^2}{2M_I} + \hat{V}(\underline{\mathbf{r}},\underline{\mathbf{R}}), \quad (6)$$

where the first line describes the electronic and photonic Hamiltonian, and the second line the nuclear Hamiltonian including $\hat{V}$ that contains all electron-nuclear and nuclear-nuclear interactions. We will for now not specify $\hat{V}$, but only specify it in the actual application. We proceed by defining the photonic Hamiltonian as

$$\hat{H}_p = \sum_{\alpha=1}^{\mathcal{N}}\frac{1}{2}\left[\hat{p}_\alpha^2 + \omega_\alpha^2\left(\hat{q}_\alpha + \frac{\boldsymbol{\lambda}_\alpha}{\omega_\alpha}\cdot\hat{\boldsymbol{\mu}}\right)^2\right], \quad (7)$$

with the total dipole moment of the system $\hat{\boldsymbol{\mu}} = \sum_{I=1}^{K} Z_I\mathbf{R}_I - \sum_{i=1}^{n_e}\mathbf{r}_i$.

We now demonstrate that QEDFT can be extended to include nuclear systems using an extension of the Runge-Gross theorem to arbitrary multicomponent systems [31] that has been applied to electron and nuclei coupled systems [30].

Every density-functional theory is based on a one-to-one correspondence between internal variables and external variables. Both directly follow from the external Hamiltonian given by Eq. 2. Therefore, the main formal result of this work can be illustrated by the following one-to-one correspondence that holds for a given initial state Ψ_0

$$\left(n, \mathbf{R}_I, q_\alpha\right) \underset{1:1}{\longleftrightarrow} \left(v_{\text{ext}}, \mathbf{F}_{\text{ext}}^{(I)}, j_{\text{ext}}^{(\alpha)}\right). \quad (8)$$

While the previously introduced Eqns. 1-7 define the mapping $\left(v_{\text{ext}}, \mathbf{F}_{\text{ext}}^{(I)}, j_{\text{ext}}^{(\alpha)}\right) \longrightarrow \left(n, \mathbf{R}_I, q_\alpha\right)$, the inverse mapping does not exist in general.

To show Eq. 8, we introduce the equations of motion (EOM) for the internal variables in Eq. 8. We start by discussing the EOM for the photon coordinate $q_\alpha(t)$ that is given by [16]

$$\ddot{q}_\alpha(t) + \omega_\alpha^2 q_\alpha(t) + \omega_\alpha\boldsymbol{\lambda}_\alpha\cdot\boldsymbol{\mu}(t) = -j_{\text{ext}}^{(\alpha)}(t)/\omega_\alpha. \quad (9)$$

This equation is a wave equation and identical to Maxwell's equations in the length-gauge with the external source term $-j_{\text{ext}}^{(\alpha)}(t)/\omega_\alpha$. Next, we look at the K EOM for the nuclei coordinates $\mathbf{R}_I$. We find

$$M_I\ddot{\mathbf{R}}_I(t) + \sum_{\beta=1}^{N_I}\sum_{\alpha=1}^{\mathcal{N}} Z_I\omega_\alpha\boldsymbol{\lambda}_\alpha\left(q_\alpha(t) + \frac{\boldsymbol{\lambda}_\alpha}{\omega_\alpha}\cdot\boldsymbol{\mu}(t)\right) + \sum_{\beta=1}^{N_I}\mathbf{F}_{\text{str}}^{(I,\beta)}(t) = -\sum_{\beta=1}^{N_I}\mathbf{F}_{\text{ext}}^{(I)}(t), \quad (10)$$

with the nuclear stress force $\mathbf{F}_{\text{str}}^{(I,\beta)}(t) = \langle\Psi(t)|\vec{\nabla}_{I,\beta}\hat{V}(\underline{\mathbf{r}},\underline{\mathbf{R}})|\Psi(t)\rangle$ that is by construction identical for each particle β.

The EOM for the electron density $n(\mathbf{r},t)$ is given by the following Sturm-Liouville problem

$$\ddot{n}(\mathbf{r},t) + \vec{\nabla}\cdot\mathbf{F}_{\text{str}}(\mathbf{r},t) + \sum_{\alpha=1}^{\mathcal{N}}\vec{\nabla}\cdot\mathbf{F}_\alpha(\mathbf{r},t) + \vec{\nabla}\cdot\mathbf{F}_N(\mathbf{r},t) = \vec{\nabla}\cdot\left(n(\mathbf{r},t)\vec{\nabla}v_{\text{ext}}(\mathbf{r},t)\right), \quad (11)$$

which contains force densities $F_{\text{str}/\alpha/N}(\mathbf{r},t)$ originated by the kinetic energy, electron-electron interactions, electron-photon, electron-nuclear respectively and are given by

$$\begin{aligned}\mathbf{F}_{\text{str}}(\mathbf{r},t) &= \mathrm{i}\,\langle\Psi(t)|\,[\hat{T}(\underline{\mathbf{r}}) + \hat{W}(\underline{\mathbf{r}},\underline{\mathbf{r}}'), \hat{j}_p(\mathbf{r})]\,|\Psi(t)\rangle\,,\\ \mathbf{F}_N(\mathbf{r},t) &= \mathrm{i}\,\langle\Psi(t)|\,[\hat{V}(\underline{\mathbf{r}},\underline{\mathbf{R}}), \hat{j}_p(\mathbf{r})]\,|\Psi(t)\rangle\,,\\ \mathbf{F}_\alpha(\mathbf{r},t) &= \boldsymbol{\lambda}_\alpha\,\langle\Psi(t)|\,\hat{n}(\mathbf{r})\,(\boldsymbol{\lambda}_\alpha\cdot\hat{\boldsymbol{\mu}} + \omega_\alpha\hat{q}_\alpha)\,|\Psi(t)\rangle\,.\end{aligned}$$

with the paramagnetic current operator $\hat{j}_p(\mathbf{r})$ [32]. $\hat{T}$, and $\hat{W}$ correspond to the first and second term of Eq. 6.

These coupled Eqns. 9-11 and the initial values $n(\mathbf{r},t_0)$, $\dot{n}(\mathbf{r},t_0)$, $\mathbf{R}_I(t_0)$, $\dot{\mathbf{R}}_I(t_0)$, $q_\alpha(t_0)$, and $\dot{q}_\alpha(t_0)$ represent an exact reformulation of the Schrödinger equation of Eq. 1 and therefore completely define the internal variables of Eq. 8. The uniqueness of the mapping defined in Eq. 8

can be proven under the usual TDDFT assumption of t-analyticity such that a Taylor expansion around the initial time t_0 is possible [33]. Then, we can follow closely the original TDDFT proof [34] with extensions to electron-nuclear systems [30] and QEDFT [14, 15]. We show that for given initial state Ψ_0, two different sets of external variables, i.e. $\left(v_{\text{ext}}, \mathbf{F}_{\text{ext}}^{(I)}, j_{\text{ext}}^{(\alpha)}\right)$ and $\left(v_{\text{ext}}^{'}, \mathbf{F}_{\text{ext}}^{(I)'}, j_{\text{ext}}^{(\alpha)'}\right)$ will always lead to two different sets of internal variables $(n, \mathbf{R}_I, q_\alpha)$, and $(n', \mathbf{R}'_I, q'_\alpha)$. First, we perform a Taylor-expansion of $v_{\text{ext}}(\mathbf{r}, t)$, $\mathbf{F}_{\text{ext}}^{(I)}(t)$, and $j_{\text{ext}}^{(\alpha)}(t)$ around initial time t_0 to obtain the Taylor coefficients $v_{\text{ext}}^{(k)}(\mathbf{r}, t_0)$, $\mathbf{F}_{\text{ext}}^{(I,k)}(t_0)$, and $j_{\text{ext}}^{(\alpha,k)}(t_0)$. Second, we then insert this expansion into Eqns. 9-11 to obtain the Taylor coefficients of $(n, \mathbf{R}_I, q_\alpha)$ in terms of $v_{\text{ext}}^{(k)}(\mathbf{r}, t_0)$, $\mathbf{F}_{\text{ext}}^{(I,k)}(t_0)$, and $j_{\text{ext}}^{(\alpha,k)}(t_0)$ and accordingly for the second set $(n', \mathbf{R}'_I, q'_\alpha)$. Third, assuming a minimum order of $k = k_{\text{min}}$ for which the difference of the external set does not vanish [35], we find a non-vanishing difference of $(n, \mathbf{R}_I, q_\alpha)$ and $(n', \mathbf{R}'_I, q'_\alpha)$ for $k_{\text{min}} + 2$. As a consequence, $(n, \mathbf{R}_I, q_\alpha)$ and $(n', \mathbf{R}'_I, q'_\alpha)$ will be different at $t_0 + \delta t$ [36]. Therefore two different sets of external variables will always lead to two different sets of internal variables, thus proving the mapping outlined in Eq. 8 for given initial state Ψ_0 [37].

To solve the coupled Eqns. 9-11 in practice, we need explicit expressions in terms of n, $\mathbf{R}_I$, q_α for the nuclear force $\mathbf{F}_{\text{str}}^{(I,\beta)}$ and the electronic force densities $\mathbf{F}_{\text{str}}, \mathbf{F}_N, \mathbf{F}_\alpha$. To approximate these quantities, we use a Kohn-Sham scheme, which is very successful in electronic-structure calculations (see, e.g., Refs. [30, 38]). In total, we find $n + \mathcal{N} + N_I \times K$ Kohn-Sham equations that read as follows

$$i\frac{\partial}{\partial t}\varphi_i(\mathbf{r}, t) = \left[-\frac{\vec{\nabla}_i^2}{2} + v_s(\mathbf{r}, t)\right]\varphi_i(\mathbf{r}, t) \quad (12)$$

$$M_I\ddot{\mathbf{Q}}_{I,\beta}(t) = -\mathbf{F}_s^{(I,\beta)}(t) \quad (13)$$

$$\ddot{q}_\alpha(t) + \omega_\alpha^2 q_\alpha(t) = -j_s^{(\alpha)}(t)/\omega_\alpha, \quad (14)$$

where we have to choose the same initial conditions, i.e. $n(\mathbf{r}, t_0) = \sum_{i=1}^{n_e}\varphi_i^*(\mathbf{r}, t_0)\varphi_i(\mathbf{r}, t_0)$, $\dot{n}(\mathbf{r}, t_0)$, $\mathbf{R}_I(t_0) = \sum_{\beta=1}^{N_I}\mathbf{Q}_{I,\beta}(t_0)$, $\dot{\mathbf{R}}_I(t_0)$, and $q_\alpha(t_0)$, $\dot{q}_\alpha(t_0)$, as in the physical system. For the photons subsystem we find

$$j_s^{(\alpha)}(t) = \omega_\alpha^2\boldsymbol{\lambda}_\alpha \cdot \boldsymbol{\mu}(t) + j_{\text{ext}}^{(\alpha)}(t). \quad (15)$$

where all terms are explicitly known. We depict a schematic illustration of the proposed scheme in Fig. S1.

In Eq. 13, we have introduced Kohn-Sham trajectories $\mathbf{Q}_{I,\beta}$ for every single nucleus in the system. However, if we have indistinguishable particles, only the total trajectory $\mathbf{Q}_I$ of that species is observable. In this way, the nuclear force $\mathbf{F}_s^{(I)}(t)$ is defined such that the sum of all Kohn-Sham trajectories $\mathbf{Q}_{I,\beta}$ reproduces the exact total trajectory of that species, i.e. $\mathbf{R}_I(t) = \sum_{\beta=1}^{N_I}\mathbf{Q}_{I,\beta}(t)$. This way we define

$$\mathbf{F}_s^{(I,\beta)}(t) = \sum_{\alpha=1}^{\mathcal{N}} Z_I\omega_\alpha\boldsymbol{\lambda}_\alpha\left(q_\alpha(t) + \frac{\boldsymbol{\lambda}_\alpha}{\omega_\alpha}\cdot\boldsymbol{\mu}(t)\right) + \mathbf{F}_{\text{Mxc}}^{(I,\beta)}(t) + \mathbf{F}_{\text{ext}}^{(I)}(t), \quad (16)$$

where the sum of $\mathbf{F}_{\text{Mxc}}^{(I,\beta)}(t)$ is defined as $\sum_{\beta=1}^{N_I}\mathbf{F}_{\text{Mxc}}^{(I,\beta)}(t) = \sum_{\beta=1}^{N_I}\mathbf{F}_{\text{str}}^{(I,\beta)}(t)$ describes the Mean-field exchange-correlation (Mxc) contribution [39]. For the electronic Kohn-Sham system, we define the following Kohn-Sham potentials

$$v_s(\mathbf{r}, t) = v_{\text{ext}}(\mathbf{r}, t) + v_{\text{Mxc}}(\mathbf{r}, t) \quad (17)$$

with the Mxc potential

$$v_{\text{Mxc}}(\mathbf{r}, t) = v_{\text{Hxc}}(\mathbf{r}, t) + \sum_{\alpha=1}^{\mathcal{N}} v_{\text{Mxc}}^{(\alpha)}(\mathbf{r}, t) + v_{\text{Mxc}}^{(N)}(\mathbf{r}, t),$$

where these potentials are exactly defined in terms of Sturm-Liouville equations

$$\vec{\nabla}\cdot\left(n(\mathbf{r}, t)\vec{\nabla}v_{\text{Hxc}}(\mathbf{r}, t)\right) = \vec{\nabla}\cdot\left(\mathbf{F}_{\text{str}}^{(s)}(\mathbf{r}, t) - \mathbf{F}_{\text{str}}(\mathbf{r}, t)\right), \quad (18)$$

$$\vec{\nabla}\cdot\left(n(\mathbf{r}, t)\vec{\nabla}v_{\text{Mxc}}^{(\alpha)}(\mathbf{r}, t)\right) = \vec{\nabla}\cdot\mathbf{F}_\alpha(\mathbf{r}, t), \quad (19)$$

$$\vec{\nabla}\cdot\left(n(\mathbf{r}, t)\vec{\nabla}v_{\text{Mxc}}^{(N)}(\mathbf{r}, t)\right) = \vec{\nabla}\cdot\mathbf{F}_N(\mathbf{r}, t). \quad (20)$$

Over the last decades, the electronic-structure community has developed a large selection of possible approximations to the exchange-correlation (xc) potential [40]. In contrast, the nascent field of QEDFT has not yet seen the same development of approximations, so far only the one-photon optimized-effective potential (OEP) has been successfully used [17, 18]. Other possibilities are a parameterization along the lines of the local-density approximation (LDA) [41] in TDDFT. As being closely linked to QEDFT, the present formalism also allows to connect to the OEP [42] route that seems promising in the limit of weak electron-nuclear correlations.

Next, we specify the electron-nuclear potential $\hat{V}$ in Eq. 6 as [30]

$$\hat{V}(\underline{\mathbf{r}}, \underline{\mathbf{R}}) = \frac{1}{2}\sum_{I=1}^{K}\sum_{\beta=1}^{N_I}\sum_{J=1}^{K}\sum_{\substack{\gamma=1\\(J\gamma\neq I\beta)}}^{N_J}\frac{Z_I Z_J}{|\mathbf{R}_{I,\beta} - \mathbf{R}_{J,\gamma}|} - \sum_{i=1}^{n_e}\sum_{I=1}^{K}\sum_{\beta=1}^{N_I}\frac{Z_I}{|\mathbf{r}_i - \mathbf{R}_{I,\beta}|}, \quad (21)$$

where the first line describes the nuclear-nuclear interaction, while the second line describes the electron-nuclear interaction. For systems, where the overlap of nuclear wave functions remains small, such as molecular vibrations, we

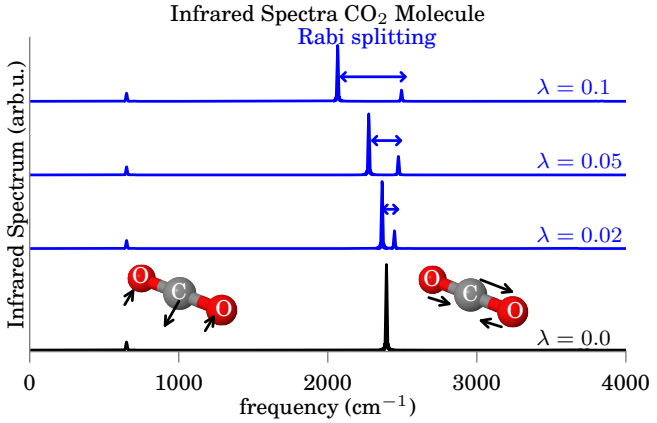

FIG. 1. **Infrared spectra in vibrational strong coupling for CO_2.** Black spectrum refers to the spectrum outside the cavity. We explicitly depict the two infrared-active vibrational modes of the CO_2 molecule. Blue spectra correspond to the electron-nuclear spectrum. Importantly, we capture the Rabi splitting between the lower and upper polariton branch.

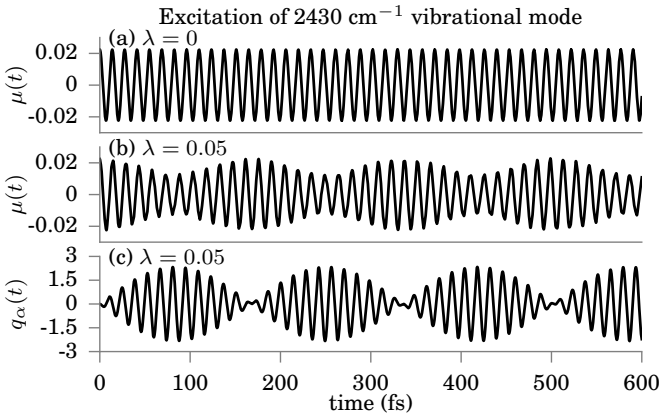

FIG. 2. **Vibrational excitation at 2430 cm^{-1}.** Initial displacement of the C-atom of $0.01\mathring{A}$, (a) dipole moment CO_2 outside the cavity, (b) dipole moment CO_2 under strong light-matter coupling for $\lambda_\alpha = 0.05$, (c) the photon displacement coordinate $q_\alpha(t)$ as defined in Eq. 5 for $\lambda_\alpha = 0.05$.

use the following approximation [30] which can be used in Eq. 13

$$\mathbf{F}_{\mathrm{M}}^{(I,\beta)}(t) = \sum_{J=1}^{K} \sum_{\substack{\gamma=1 \\ (J\gamma \neq I\beta)}}^{N_J} \frac{Z_I Z_J (\mathbf{Q}_{J,\gamma} - \mathbf{Q}_{I,\beta})}{|\mathbf{Q}_{I,\beta} - \mathbf{Q}_{J,\gamma}|^3} - \int d\mathbf{r} \frac{Z_I n(\mathbf{r},t)\,(\mathbf{r} - \mathbf{Q}_{I,\beta})}{|\mathbf{r} - \mathbf{Q}_{I,\beta}|^3}. \tag{22}$$

This force depends explicitly on the individual nuclear trajectory $\mathbf{Q}_{I,\beta}$ and therefore is similar to the self-interaction correction (SIC) of DFT [30]. Using this equation, we recover the Ehrenfest scheme [43], i.e. a mixed quantum-classical scheme that treats the electrons quantum mechanically coupled to classical nuclei. Analogously, the electron-nuclear potential follows as

$$v_{\mathrm{M}}^{(N)}(\mathbf{r},t) = -\sum_{I=1}^{K} \sum_{\beta=1}^{N_I} \frac{Z_I}{|\mathbf{r} - \mathbf{Q}_{I,\beta}(t)|}. \tag{23}$$

We now apply the presented formalism to vibrational strong-coupling of light to a molecular system (CO_2 molecule) [44] We find for CO_2 three infrared(IR)-active vibrational excitations, that are shown in Fig. 1 in black, one at 2430 cm^{-1} and the second one with a two-fold degeneracy at 654 cm^{-1} (experimental results are 2350 cm^{-1} and 667.5 cm^{-1} [45], respectively). To obtain the infrared spectra, we initially excite the three vibrational modes such that the carbon atom is displaced by $0.01\mathring{A}$ in all three spatial directions and record the time-evolution of the total dipole moment $\boldsymbol{\mu}(t)$ for 5 ps. The Fourier transform of the dipole moment yields then the infrared spectrum [43]. In Fig. 1, we also depict for all IR active modes their normal mode oscillation. If the molecule is strongly coupled to a cavity mode, we find Rabi splitting in the infrared spectra emerging. To simulate vibrational strong coupling, we choose the cavity frequency $\omega_\alpha = 2430\,\mathrm{cm}^{-1}$ in resonance to the vibrational excitation at 2430 cm^{-1} with polarization in x-direction. By varying the matter-photon coupling parameter $\lambda_\alpha = |\boldsymbol{\lambda}_\alpha|$, we can tune the system from the weak to the strong coupling limit. In Fig. 1, we show in blue the spectra for $\lambda_\alpha = (0.02, 0.05, 0.1)$ and find the Rabi-splitting occurring with increasing splitting for stronger λ_α. Next, to analyze the dynamics of the system under vibrational strong light-matter coupling in more detail, we initially displace the carbon molecule by $0.01\mathring{A}$ to specifically excite the 2430 cm^{-1} vibration. In Fig. 2 (a), we show the time-dependent dipole moment of the system under that initial excitation for up to 600 fs without matter-photon coupling. The system oscillates very regularly with a frequency of 2430 cm^{-1}. If we choose $\lambda_\alpha = 0.05$, we find an additional frequency occurring as an envelope that corresponds to the Rabi splitting as shown in Fig. 2 (b). In (c), we show a new observable that is now possible to calculate with this novel formalism. We depict the time-evolution of the photon displacement coordinate and find additionally to the regular oscillation an envelope given by the Rabi splitting. In the last example, we study in this paper, we initialize the three nuclei with random velocities drawn from a Maxwell-Boltzmann distribution corresponding to $T = 100$ K. The infrared spectrum of this run depicted in Fig. 3 shows not the same clean signature of the Rabi splitting as in Fig. 1-2 but rather a broadband with many peaks around 2430 cm^{-1}, although the cavity mode is in resonance to that frequency. Due to the initial random velocities, the molecule is spinning during the simulation time and thus the effective interaction strength $\lambda_{\alpha,\mathrm{eff}}(t) = \mathbf{e}_\alpha \cdot \boldsymbol{\mu}(t)$ changes in time. In the center of Fig. 3, we show the expectation value of $q_\alpha(t)$.

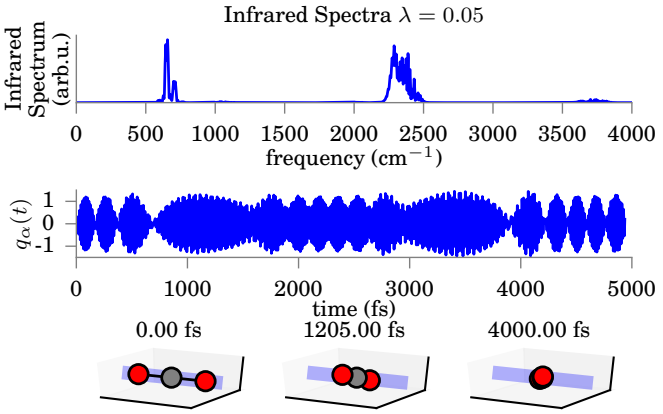

FIG. 3. **Spinning molecule.** From top to bottom: Infrared spectrum after 5 ps for a CO_2 molecule under strong-light matter coupling with $\lambda_\alpha = 0.05$. Center: time-evolution of the expectation value of $q_\alpha(t)$. Bottom: Snapshots of the nuclear positions of the spinning molecule for $t = (0, 1205, 4000)$ fs. The blue area indicates the polarization direction of the photon mode.

Although we also find an envelope that is a fingerprint of Rabi oscillations, in contrast to Fig. 2, we do not find a regular envelope function. This can be understood by looking at the atoms coordinates during the run as plotted in the bottom of Fig. 3 for $t = (0, 1205, 4000)$ fs (and as a movie in the SI). Since the molecule spins around its center of mass, we find that $\lambda_{\alpha,\text{eff}}(t) \in [0, 0.05]$. This directly translates into the spectra that exhibits a broadband of peaks at 2430 cm^{-1}.

In our work, we have demonstrated a new density-functional theory-based approach to treat the correlated electron-nuclear-photon problem. The Runge-Gross proof of QEDFT has been extended to the realm of nuclear motion, and we have applied this new theoretical method to analyze vibrational strong coupling, of high relevance to experimental work in this field. Our calculations are the first *ab initio* calculations of vibrational strong coupling in cavities with observables that quantitatively connect with the new fields of polaritonic chemistry [46] and nanoplasmonics [1, 47] that are pushing the envelope in strong light-matter interactions. Future directions include the *ab initio* study of chemical reactions using quantum transition state theory [48] within the framework of polaritonic chemistry [46] that have recently been demonstrated experimentally [6] and are now within computational reach. to study excited-state phenomena [49] of vibrationally strongly-coupled cavity systems within a linear-response formalism, and the study of the rotational-vibrational sidebands under strong light-matter coupling. We envision using this understanding of quantum-cavity controlled vibrational strong coupling as a testbed to develop a general methodology for optical control of chemical dynamics via strong light-matter coupling to alter the fundamental pathways of molecular species, and by accessing matter-photon correlations, creating a new method of quantum correlated spectroscopy.

We thank Nick Rivera, and Michael Ruggenthaler for fruitful discussions, and George Varnavides for graphical support. We acknowledge support from the STC Center for Integrated Quantum Materials NSF grant number DMR-1231319 and from the Harvard John A. Paulson School of Engineering and Applied Sciences. JF acknowledges financial support from the Deutsche Forschungsgemeinschaft (DFG) under Contract No. FL 997/1-1.

* Electronic address: flick@seas.harvard.edu
† Electronic address: prineha@seas.harvard.edu

[1] F. Benz, M. K. Schmidt, A. Dreismann, R. Chikkaraddy, Y. Zhang, A. Demetriadou, C. Carnegie, H. Ohadi, B. de Nijs, R. Esteban, J. Aizpurua, and J. J. Baumberg, Science **354**, 726 (2016).
[2] J. George, T. Chervy, A. Shalabney, E. Devaux, H. Hiura, C. Genet, and T. W. Ebbesen, Phys. Rev. Lett. **117**, 153601 (2016).
[3] H. Memmi, O. Benson, S. Sadofev, and S. Kalusniak, Phys. Rev. Lett. **118**, 126802 (2017).
[4] A. Shalabney, J. George, H. Hiura, J. A. Hutchison, C. Genet, P. Hellwig, and T. W. Ebbesen, Angewandte Chemie **127**, 8082 (2015).
[5] A. Canaguier-Durand, E. Devaux, J. George, Y. Pang, J. A. Hutchison, T. Schwartz, C. Genet, N. Wilhelms, J.-M. Lehn, and T. W. Ebbesen, Angewandte Chemie **125**, 10727 (2013).
[6] A. Thomas, J. George, A. Shalabney, M. Dryzhakov, S. J. Varma, J. Moran, T. Chervy, X. Zhong, E. Devaux, C. Genet, J. A. Hutchison, and T. W. Ebbesen, Angewandte Chemie International Edition **55**, 11462 (2016).
[7] F. Herrera and F. C. Spano, Phys. Rev. Lett. **116**, 238301 (2016).
[8] M. A. Zeb, P. G. Kirton, and J. Keeling, ACS Photonics **5**, 249 (2018), https://doi.org/10.1021/acsphotonics.7b00916.
[9] J. Feist, J. Galego, and F. J. Garcia-Vidal, ACS Photonics **5**, 205 (2018), https://doi.org/10.1021/acsphotonics.7b00680.
[10] J. Flick, M. Ruggenthaler, H. Appel, and A. Rubio, Proceedings of the National Academy of Sciences **114**, 3026 (2017), http://www.pnas.org/content/114/12/3026.full.pdf.
[11] M. Ruggenthaler, N. Tancogne-Dejean, J. Flick, H. Appel, and A. Rubio, Nature Reviews Chemistry **2**, 0118 (2018).
[12] L. A. Martínez-Martínez, R. F. Ribeiro, J. Campos-González-Angulo, and J. Yuen-Zhou, ACS Photonics **5**, 167 (2018), https://doi.org/10.1021/acsphotonics.7b00610.
[13] M. Ruggenthaler, F. Mackenroth, and D. Bauer, Phys. Rev. A **84**, 042107 (2011).
[14] I. V. Tokatly, Phys. Rev. Lett. **110**, 233001 (2013).
[15] M. Ruggenthaler, J. Flick, C. Pellegrini, H. Appel, I. V. Tokatly, and A. Rubio, Phys. Rev. A **90**, 012508 (2014).
[16] J. Flick, M. Ruggenthaler, H. Appel, and A. Rubio, Proc. Natl. Acad. Sci. U. S. A. **112**, 15285 (2015), http://www.pnas.org/content/112/50/15285.full.pdf.
[17] C. Pellegrini, J. Flick, I. V. Tokatly, H. Appel, and A. Rubio, Phys. Rev. Lett. **115**, 093001 (2015).

[18] J. Flick, C. Schäfer, M. Ruggenthaler, H. Appel, and A. Rubio, ACS Photonics **5**, 992 (2018), https://doi.org/10.1021/acsphotonics.7b01279.

[19] J. Flick, H. Appel, M. Ruggenthaler, and A. Rubio, Journal of Chemical Theory and Computation **13**, 1616 (2017), pMID: 28277664, http://dx.doi.org/10.1021/acs.jctc.6b01126.

[20] J. F. Capitani, R. F. Nalewajski, and R. G. Parr, The Journal of Chemical Physics **76**, 568 (1982), https://doi.org/10.1063/1.442703.

[21] T. Kreibich and E. K. U. Gross, Phys. Rev. Lett. **86**, 2984 (2001).

[22] T. Kreibich, R. van Leeuwen, and E. K. U. Gross, Phys. Rev. A **78**, 022501 (2008).

[23] A. Chakraborty, M. V. Pak, and S. Hammes-Schiffer, Phys. Rev. Lett. **101**, 153001 (2008).

[24] A. Sirjoosingh and S. Hammes-Schiffer, The Journal of Physical Chemistry A **115**, 2367 (2011), pMID: 21351757, http://dx.doi.org/10.1021/jp111210c.

[25] S. Baroni, S. de Gironcoli, A. Dal Corso, and P. Giannozzi, Rev. Mod. Phys. **73**, 515 (2001).

[26] R. Requist and E. K. U. Gross, Phys. Rev. Lett. **117**, 193001 (2016).

[27] F. Giustino, Rev. Mod. Phys. **89**, 015003 (2017).

[28] Other possible approaches include exact factorization [**? ? ?**], path integrals [**?**], and perturbative theory [25, 27].

[29] D. Craig and T. Thirunamachandran, *Molecular Quantum Electrodynamics: An Introduction to Radiation-molecule Interactions*, Dover Books on Chemistry Series (Dover Publications, 1998).

[30] E. K. U. Gross, J. F. Dobson, and M. Petersilka, "Density functional theory of time-dependent phenomena," in *Density Functional Theory II: Relativistic and Time Dependent Extensions*, edited by R. F. Nalewajski (Springer Berlin Heidelberg, Berlin, Heidelberg, 1996) pp. 81–172.

[31] T.-C. Li and P.-q. Tong, Phys. Rev. A **34**, 529 (1986).

[32] M. Ruggenthaler and R. van Leeuwen, EPL (Europhysics Letters) **95**, 13001 (2011).

[33] More general proofs [**?**] may be formulated along the lines of Refs. [32**?**].

[34] E. Runge and E. K. U. Gross, Phys. Rev. Lett. **52**, 997 (1984).

[35] $k_{\min}$ exists, since the potentials are different by construction.

[36] Provided the initial density $n(\mathbf{r}, t_0)$ is reasonably well behaved [34**?**], the last step can be shown by *reductio ad absurdum* [34**?**].

[37] Up to a time-dependent scalar function $c(t)$ in $v_{\text{ext}}(\mathbf{r}, t)$.

[38] W. Kohn, Rev. Mod. Phys. **71**, 1253 (1999).

[39] For Fröhlich coupling [27], we find a vanishing xc contribution.

[40] M. A. Marques, M. J. Oliveira, and T. Burnus, Computer Physics Communications **183**, 2272 (2012).

[41] W. Kohn and L. J. Sham, Phys. Rev. **140**, A1133 (1965).

[42] S. Kümmel and L. Kronik, Rev. Mod. Phys. **80**, 3 (2008).

[43] X. Andrade, A. Castro, D. Zueco, J. L. Alonso, P. Echenique, F. Falceto, and Á. Rubio, Journal of Chemical Theory and Computation **5**, 728 (2009), pMID: 26609578, https://doi.org/10.1021/ct800518j.

[44] See Supplemental Material for the numerical details of our implementation, which includes Refs. [**? ? ?**].

[45] P. E. Martin and E. F. Barker, Phys. Rev. **41**, 291 (1932).

[46] T. W. Ebbesen, Accounts of Chemical Research **49**, 2403 (2016).

[47] J. Mertens, M.-E. Kleemann, R. Chikkaraddy, P. Narang, and J. J. Baumberg, Nano Letters **17**, 2568 (2017), pMID: 28267346, http://dx.doi.org/10.1021/acs.nanolett.7b00332.

[48] S. Shin and H. Metiu, J. Chem. Phys. **102**, 9285 (1995).

[49] J. Flick, D. M. Welakuh, M. Ruggenthaler, H. Appel, and A. Rubio, arXiv preprint arXiv:1803.02519 (2018).